Colloid Polym Sci (2015) 293:833–840
DOI 10.1007/s00396-014-3470-y

ORIGINAL CONTRIBUTION

Dielectric analysis on the phase behavior of ionic liquid-containing nonaqueous microemulsions

Kai Chen · Kongshuang Zhao

Received: 10 August 2014 / Revised: 15 October 2014 / Accepted: 21 November 2014 / Published online: 4 December 2014

Abstract The phase behavior of 1-butyl-3-methylimidazolium hexafluorophosphate ([Bmim][PF_6], a hydrophobic ionic liquid (IL)), polyethylene glycol p-(1,1,3,3-tetramethylbutyl)-phenyl ether (Triton X-100, a nonionic surfactant with a polyoxyethylene chain), and ethylene glycol (EG) ternary nonaqueous systems, was studied by dielectric relaxation spectroscopy (DRS). In single-phase region, EG-in-IL (EG/IL), bicontinuous (B.C.), and IL-in-EG (IL/EG) subregions can be identified by the dc conductivity. The inflection points of the relaxation parameters (dielectric intensity and relaxation time) are consistent with the phase boundaries between IL/EG and B.C. and B.C. and EG/IL subregions, which imply that the change of microstructure of this system can be detected by the dielectric response. Furthermore, in IL/EG microregion, phase parameters of constituent phases were calculated based on interface polarization theory. The trends of relaxation times for both of the calculated values τ_{MW} and experimental values τ as a function of IL content in IL/EG microregion are almost the same, which infers that the dielectric relaxation originates from the interfacial polarization. This work is helpful to understand the dynamics and phase behavior of nonaqueous microemulsions.

Keywords Nonaqueous microemulsions · Ionic liquid · Dielectric study · Phase behavior · Interfacial polarization

Introduction

Microemulsions are thermodynamically stable, isotropic, transparent colloidal solutions, consisting of three components: a surfactant (amphiphile), a polar solvent (usually water), and a nonpolar solvent (oil). Generally, the majority of studies in microemulsions utilize water as polar component [1]. However, there are many chemical reactions requiring water-free environment. To solve this problem, attempts have been made to prepare and study nonaqueous microemulsions, where water has been replaced by polar organic solvents (such as ethylene glycol (EG), propylene glycol (PG), glycerol (GY), formamide (FA), and dimethylformamide (DMF)) [2–8]. These nonaqueous microemulsions have a number of distinct advantages over aqueous ones, especially when used as media for chemical reactions that need to avoid contact with water, such as Diels–Alder reaction [7], esterification/transesterification [9], and polymerization [10].

Recently, nonaqueous microemulsions using ionic liquids (ILs, molten salts that generally consist of organic cations and organic/inorganic anions) as a substitute for organic solvents or water have become an interesting topic [11, 12]. These ILs-containing microemulsions systems have attracted interest from both a fundamental and a practical perspective, since they cannot only overcome solubility limitations of ILs in immiscible solvents but also improved the properties of microemulsions significantly [13, 14]. Varied techniques have been applied to study the properties and features of these microemulsions systems, such as [15–18], small-angle X-ray scattering [19–21], electrochemical cyclic voltammetry [17, 22], microcalorimetry [23], dynamic light scattering [16, 18, 24, 25], ultraviolet visible techniques [24], freeze-fracture electron microscopy [26, 27], etc. Although these systems have been intensively investigated, their dynamics and phase behavior features are still not very clear.

Dielectric relaxation spectroscopy (DRS), which usually measures permittivity and conductivity as a function of frequency, has become one of the powerful methods to study microstructure and dynamics of microemulsions in the last two decades [28–41]. In these studies, the information on

K. Chen · K. Zhao (✉)
College of Chemistry, Beijing Normal University, Beijing 100875, China
e-mail: zhaoks@bnu.edu.cn

dynamics process of aqueous microemulsions in extremely wide frequency range and over large interval of temperature and composition has been mostly well studied [29–39], but little attention has been paid to nonaqueous microemulsions [40, 41]. Particularly, the influence of IL content on the structure and dynamics of nonaqueous microemulsions has not been investigated by the well-established dielectric theory.

In this work, we employed DRS to study phase behavior of EG/p-(1,1,3,3-tetramethylbutyl) phenoxypolyoxyethyleneglycol (Triton X-100)/ 1-butyl-3-methylimidazolium hexafluorophosphate ([Bmim][PF_6]) ternary nonaqueous microemulsions system. In order to clarify the relationship between structural transformation and composition of the systems, the dependence of conductivity on IL contents was discussed. By further study of the dielectric properties of difference phases, exact boundaries of the phase diagram have been clarified and the dynamics behavior has been discussed. Moreover, we also acquire some internal properties of the constituent phases through analyzing the dielectric parameters with appropriate theoretical model.

Experimental

Preparation of microemulsions

Triton X-100 (p-(1,1,3,3-tetramethylbutyl)phenoxypoly oxyethyleneglycol) (A.R. grade) used in this work was purchased from Amresco Chemical Inc. America. 1-butyl-3-methylimidazolium hexafluorophosphate ([Bmim][PF_6]) (purity >99.2 %) was purchased from Shanghai Cheng Jie Chemical Co., China. Ethylene glycol (EG) (A.R. grade) was obtained from Beijing Chemical Works. The structures of Triton X-100 and [Bmim][PF_6] were shown in Fig. 1. They were dried under vacuum at 80 °C for 12 h before use.

The microemulsions were prepared by mixing EG, Triton X-100, and [Bmim][PF_6] in appropriate weight fractions. The mixtures of EG/Triton X-100/[Bmim][PF_6] were prepared in accordance with the phase diagram of this ternary system at 30.0 °C [26]. The experimental path is shown in Fig. 2, which illustrates the increase of the weight fraction of IL (*W*t%(IL)) ranging from 0 to 37.5 % when the weight fraction of Triton

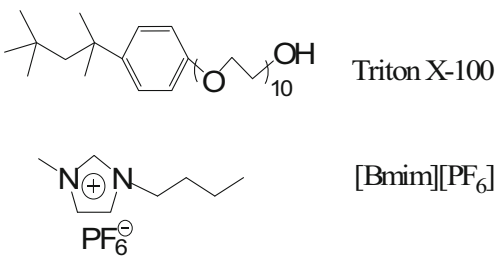

Fig. 1 Chemical structure of Triton X-100 and [Bmim][PF_6]

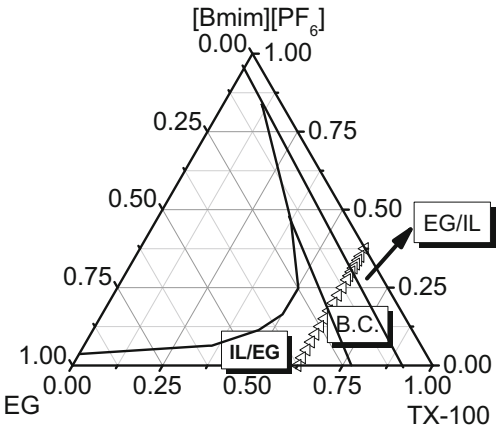

Fig. 2 Experimental path (*triangle*) in this work for EG/Triton X-100/[Bmim][PF6] systems. The path denotes the change of IL content in the ternary systems when the weight ratio of Triton X-100 was fixed as 62.5 %; the phase diagram at 30.0 °C is cited from reference [26]

X-100 was fixed to 62.5 %. According to the phase diagram, it can be seen that the path crosses three different subregions, i.e., this ternary mixture was in the IL-in-EG (IL/EG) microemulsion phase when *W*t%(IL)≤18.0 %, in the bicontinuous (B.C.) phase when 18.0 %<*W*t %(IL)<30.0 %, and in the EG-in-IL (EG/IL) microemulsion phase when *W*t %(IL)≥30.0 %.

Dielectric Measurements

The dielectric measurements were performed on a 4294A precision impedance analyzer (Agilent Technologies) that allowed a continuous frequency measurement from 40 Hz to 110 MHz. A dielectric measurement cell with concentrically cylindrical platinum electrodes was employed and connected to the impedance analyzer by a 1607E spring clip fixture. The amplitude of the applied alternating field was 500 mV, and the measurement temperature was (30± 0.5 °C). In order to submerge the electrodes, the mass of solutions used in the experiment was 2.0 g. The experimental data errors arising from the residual inductance and measurement cell were corrected by Schwan's method [42]. The cell constant C_l, stray capacitance C_r, and residual inductance L_r that have been determined by several standard substances (air, pure ethanol, and pure water) were 0.45 pF, 3.17 pF, and 1.13×10^{-8} F/S^2, respectively. The permittivity and total dielectric loss at each measured frequency were calculated from the corrected capacitance and conductance.

Determination of dc conductivity and relaxation parameters

In an applied electric field of frequency *f*, the dielectric properties (permittivity ε and conductivity κ) of microemulsions

can be obtained by fitting the Cole–Cole empirical equation [43] (Eq. (1)) to the experimental data:

$$\varepsilon^* = \varepsilon' - j\varepsilon'' = \varepsilon_h + \sum_i \frac{\varepsilon_l - \varepsilon_h}{1 + (j\omega\tau_i)^{\beta}} \quad (1)$$

where ε^* is the complex permittivity, ε' is the permittivity, ε'' is the dielectric loss, i is the number of the dielectric relaxation, $\Delta\varepsilon(=\varepsilon_l-\varepsilon_h)$ is the relaxation intensity, ε_l and ε_h are the low- and high-frequency limits of relative permittivity, respectively, ω is the angular frequency ($\omega=2\pi f$, f is the frequency), τ is the relaxation time, β ($0<\beta\leq 1$) is the Cole–Cole parameter indicating the dispersion of the relaxation time τ, and $j^2=-1$. $\varepsilon''=(\kappa-\kappa_l)/\omega\varepsilon_0$, and $\tau=(2\pi f_0)^{-1}$ in which κ is the conductivity, κ_l is the low-frequency limit of conductivity (which can be estimated from the scaling dependence of total dielectric loss with a slope −1 on ω), ε_0 is the permittivity of vacuum equal to 8.854×10^{-12} F/m^{-1}, and f_0 is the characteristic frequency.

A considerable electrode polarization (EP) effect dominates in the frequency range below 10^6 Hz due to the existence of [Bmim][PF_6] in this microemulsions system. The electrode polarization term (ε_{EP}) is expressed as $\varepsilon_{EP}=A\omega^{-m}$. To acquire accurate values of dielectric parameters, the electrode polarization term is added to the Cole–Cole equation (Eq. (1)), so the Cole–Cole equation is expressed as

$$\varepsilon^* = \varepsilon_h + \sum_i \frac{\varepsilon_l - \varepsilon_h}{1 + (j\omega\tau_i)^{\beta}} + A\omega^{-m} \quad (2)$$

where A and m are adjustable parameters. All the data were eventually fitted with (Eq. (2)). By using this method, the influence of EP can be subtracted from the experimental data, and the real dielectric response of the sample is obtained.

Results and discussion

Dielectric behaviors of microemulsions

Figure 3 shows three-dimensional representations for the frequency dependence of the permittivity and dielectric loss of these ternary systems. In Fig. 3a, the dielectric behavior of these systems seems varying smoothly as IL content increase. The dielectric loss peak locates in the vicinity of 10 MHz and shifts slightly with decreasing IL content are shown in Fig. 3b [44], which correspond to a relaxation with a relaxation time of the order of 1 ns.

To examine the dielectric spectra in detail, typical ones cut at IL contents *Wt*%(IL) at 5.0, 15.0, 25.0, and 35 % are shown in Fig. 4. The dielectric parameters (ε_l, ε_h, and τ) by fitting Eq. (2) which includes one Cole–Cole's terms (i=1) to the experimental data are listed in Table 1. The value of β has been used to forecast the shape or morphology of the microemulsions [28]. From Table 1, the value of β is about 0.76, which indicates that the isotropy of the droplet IL contents changing don't further extent [36]. The dependence of the conductivity and permittivity on IL content can reflect the structural transformation, as discussed in Sections "Conductance of microemulsions" and "Structural transition of microemulsions".

Conductance of microemulsions

Measurement of electrical conductivity is one of the powerful tools to locate the subregions of microemulsions, which can provide information about the transport of ions [18, 45, 46]. Generally, the conductivity of aqueous microemulsions shows quite a remarkable change over many orders of magnitude. This phenomenon is known as electric percolation [47–49]. However, the application of conductivity method is limited in IL microemulsions systems due to the high conductivity of ILs [17, 26]. Fortunately in our work, the dependences of dc conductivity κ_l on IL content show inflection at 18.6 and 30.0 %, which are assigned with the phase boundaries

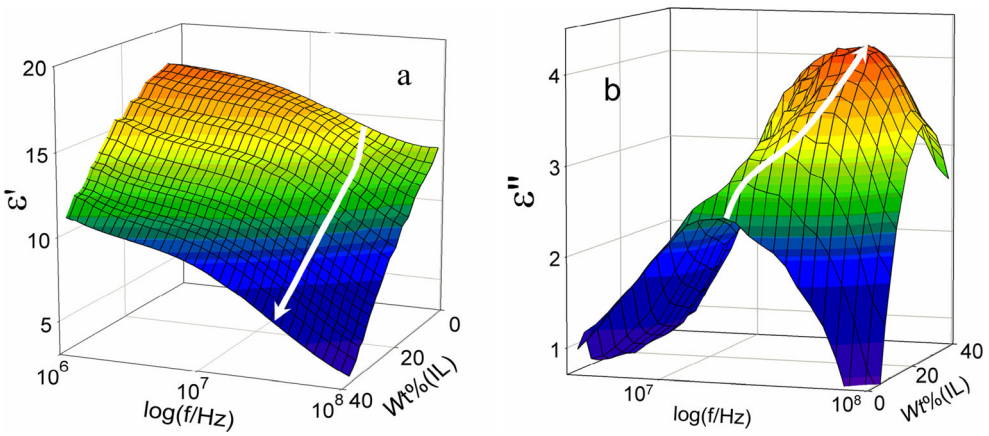

Fig. 3 Three-dimensional representations for the frequency dependence of **a** permittivity ε' and **b** dielectric loss ε'' of ternary systems of EG/Triton X-100/[Bmim][PF_6] (when the weight ratio of Triton X-100 was fixed at 62.5 %) with different IL contents. The directions of increasing weight fraction of IL are shown by the *arrows*

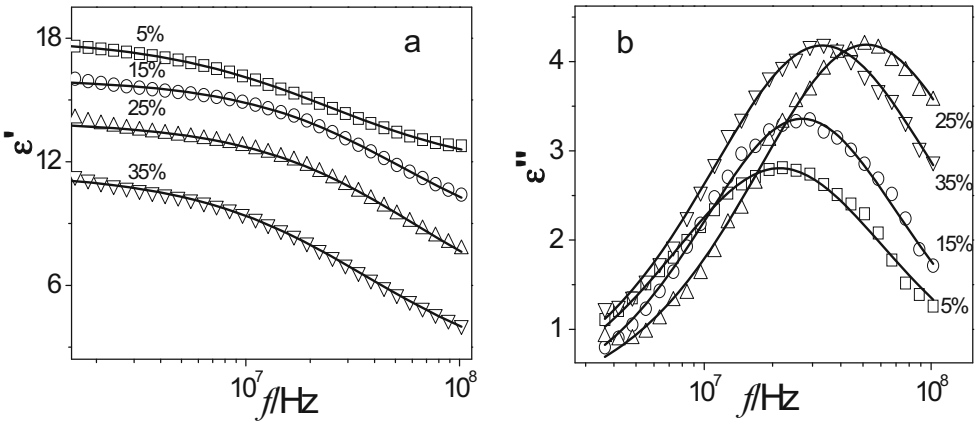

Fig. 4 The **a** dielectric permittivity ε' and **b** dielectric loss ε'' spectra extracted from Fig. 3 at several IL contents (*square*) 5 %, (*circle*) 15 %, (*up-pointing triangle*) 25 %, and (*down-pointing triangle*) 35 %, respectively. The *symbols* and the *solid lines* represent the experimental data and the best fitting curves by Eq. (2), respectively

between IL/EG and B.C. and B.C. and EG/IL subregions, respectively.

Figure 5 shows the dependence of (a) the dc conductivity κ_l (*square*), (b) the relaxation time τ (*circle*), and (c) the dielectric intensity $\Delta\varepsilon$ (*triangle*) on IL contents when the weight ratio of Triton X-100 was fixed at 62.5 %. In Fig. 5a, the value of conductivity ranges between (0.89 and 3.55)$\times 10^{-4}$ S/cm, which has the same order of magnitude as the report in literature [26]. Obviously, the main attribution to the conductance in the microemulsions results from [Bmim][PF_6]. When the IL contents *Wt*%(IL) is below 18.6 %, the conductivity increases linearly with the IL content due to the number of migrating ions ($[Bmim]^+$ and PF_6^-) increase. When the IL contents *Wt*%(IL) in the range from 18.6 to 30.0 %, the conductivity remains almost constant in B.C. region, because of the formation of EG channels and IL channels. This interpretation is supported by the previous results from freeze-fracture electron microscopy, indicating the formation of IL channels between neighboring IL droplets [26]. However, when the IL content *Wt*%(IL) is above 30.0 %, i.e., in the EG/IL subregion, the dc conductivity decreased. It was markedly different from traditional systems. Although similar trend in the conductivity versus IL content curves has been reported by other authors in water/IL/Triton X-100, they did not provide further explanation in this subregion [50]. It is well known that ILs have relatively higher viscosity than water or common organic solvents [51]. As a result, the dc conductivity begins to decrease due to the increase of viscosity which

Table 1 Dielectric parameters of EG/Triton X-100/[Bmim][PF_6] microemulsions with different IL contents when the weight ratio of Triton X-100 was fixed at 62.5 %

Wt%(IL)	ε_l	ε_h	$\Delta\varepsilon$	β	τ (ns)	κ_l ($10^4\times$S/cm)	κ_h ($10^4\times$S/cm)
2.50	18.02±0.36	12.02±0.24	6.00±0.24	0.73±0.02	7.37±0.08	0.89±0.03	1.61±0.03
5.00	18.06±0.32	11.30±0.19	6.76±0.27	0.73±0.03	6.56±0.07	1.29±0.04	2.20±0.02
7.50	17.60±0.35	10.26±0.17	7.34±0.29	0.74±0.01	4.34±0.05	1.91±0.06	3.41±0.05
10.00	17.20±0.36	9.58±0.19	7.62±0.31	0.76±0.04	3.69±0.04	2.25±0.05	4.08±0.04
12.50	16.85±0.34	8.65±0.21	8.20±0.33	0.77±0.03	3.24±0.07	2.39±0.03	4.63±0.06
15.00	16.08±0.35	7.41±0.15	8.67±0.34	0.76±0.01	2.98±0.03	2.79±0.06	5.37±0.03
17.50	15.80±0.32	6.63±0.13	9.17±0.37	0.76±0.04	2.62±0.05	3.24±0.04	6.33±0.05
20.00	14.08±0.28	4.16±0.08	9.93±0.38	0.75±0.02	2.76±0.06	3.16±0.05	6.35±0.04
22.50	14.92±0.30	5.04±0.12	9.88±0.29	0.75±0.05	2.72±0.03	3.44±0.03	6.66±0.04
25.00	14.02±0.28	3.94±0.08	10.08±0.26	0.75±0.04	2.59±0.05	3.55±0.06	6.99±0.07
27.50	13.46±0.33	3.46±0.07	10.00±0.35	0.75±0.03	2.89±0.04	3.14±0.05	6.20±0.02
28.75	13.00±0.29	2.97±0.06	10.03±0.25	0.75±0.02	2.94±0.08	3.17±0.04	6.19±0.05
30.00	12.78±0.26	2.80±0.06	9.98±0.34	0.75±0.04	3.19±0.06	2.99±0.03	5.76±0.03
31.25	12.22±0.31	2.56±0.08	9.66±0.31	0.76±0.02	3.41±0.08	2.77±0.02	5.28±0.06
32.50	11.83±0.34	2.33±0.05	9.50±0.33	0.76±0.03	3.88±0.04	2.67±0.04	4.83±0.05
33.75	11.60±0.28	2.38±0.07	9.22±0.37	0.77±0.03	4.16±0.05	2.43±0.05	4.39±0.02
35.00	11.33±0.23	2.21±0.08	9.12±0.36	0.78±0.01	5.01±0.06	2.64±0.04	4.25±0.04
37.50	10.60±0.31	1.90±0.06	8.70±0.35	0.79±0.04	5.66±0.07	2.43±0.06	3.79±0.06

κ_h the high-frequency limit of conductivity

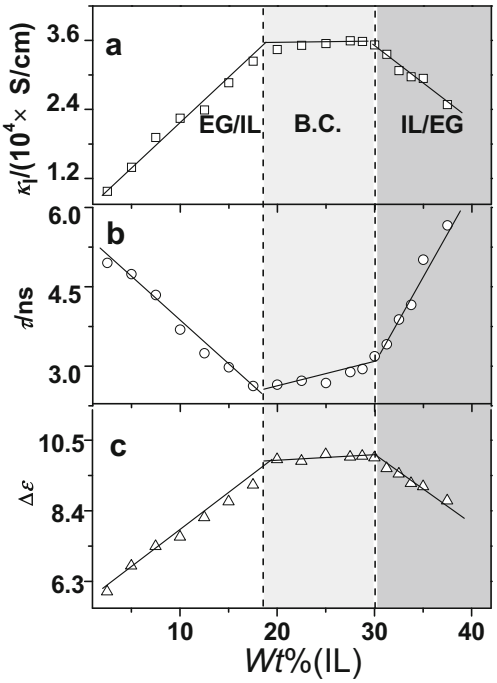

Fig. 5 Dependence of **a** the dc conductivity κ_l (*square*), **b** the relaxation time τ (*circle*), and **c** the dielectric intensity $\Delta\varepsilon$ (*triangle*) on IL contents when the weight ratio of Triton X-100 was fixed at 62.5 %. The areas filled with different color represent different phase regions. The *dashed line* shows the inflection point, and the *solid lines* are used for guiding the eyes

might decrease the rate of migration. The microstructures and phase transformation compared to traditional microemulsions are obtained by dynamic light scattering and freeze-fracture electron microscopy [26], which is observed in this work by electrical conductivity. A plausible structure of the IL/EG (a) and EG/IL (b) microemulsion is proposed in Fig. 6.

Dynamics of microemulsions

It is well known that the relaxation time τ is the most effective criterion to determine the relaxation dynamics. In general, the relaxation time τ is related to interfacial information about subregion of microemulsions. It is obvious from Fig. 5b that τ increases from about 2 to 6 ns with the increment of the IL content, which has the same order of magnitude as the report in literature [38]. When the IL content below 18.6 %, the relaxation time decreases linearly with the IL content due to the number of migrating ions ($[Bmim]^+$ and PF_6^-) increase. The value of τ remains almost constant in the B.C. subregion (i.e., the IL content in the range from 18.6 to 30.0 %), which probably because the change of sum interface is not obvious in the region. The formation of a bicontinuous structure consisting of EG and IL tunnels contributes to ion movement in this subregion. In the IL/EG region (i.e., the IL content exceeds 30.0 %), τ sharply increases with the IL contents due to the increase of viscosity, which might decrease the rate of migration. It is can be seen that three phase regions were identified by the relaxation time. The dynamics of IL-containing nonaqueous microemulsions have a similar feature in aqueous microemulsions [39, 52].

Electrical parameters of IL/EG subregion

To further investigate the detailed information about the structure of microemulsions, the effect of IL content on electrical properties of constituent phase was studied. Han et al. [26] have already observed the spherical structure of IL/EG subregions by TEM, which was similar to other aqueous microemulsions systems. According to Maxwell interface polarization theory, for a system composed of two phases, dielectric relaxation can be observed when these phases with different dielectric properties. The different dielectric properties between IL particles and bulk EG result in a dielectric relaxation caused by interface polarization. For the convenience of following analysis, here, we suppose the microstructures of IL/EG microemulsions as particle suspensions model (see Fig. 6a). That is, the EG spherical droplets with complex permittivity $\varepsilon_i^*(=\varepsilon_i - j\kappa_i/\omega\varepsilon_0)$ dispersed in a continuous media of permittivity $\varepsilon_a^*(=\varepsilon_a - j\kappa_a/\omega\varepsilon_0)$ in a volume fraction ϕ.

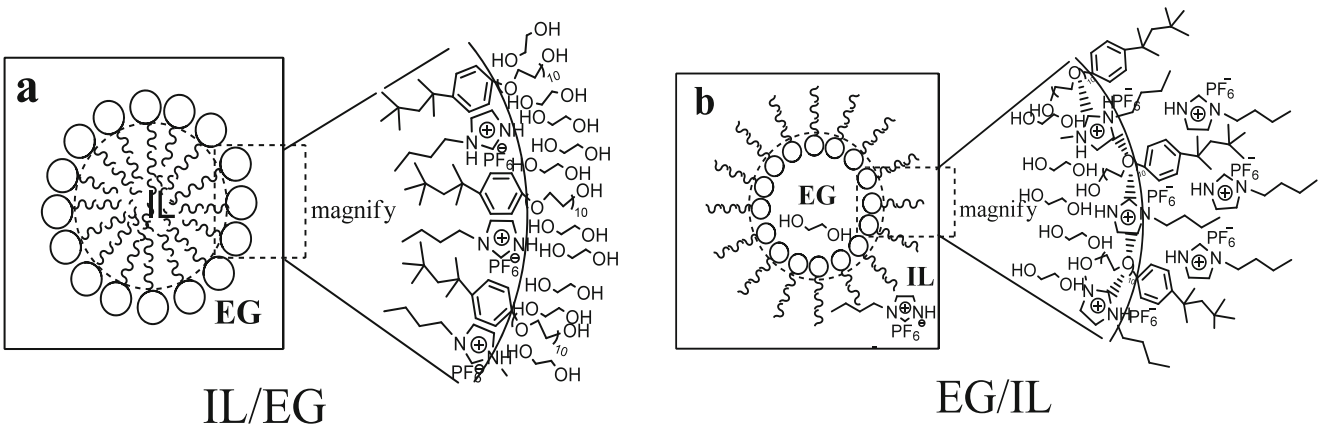

Fig. 6 Possible structure of the IL/EG (**a**) and EG/IL (**b**) microemulsions

Where ε_i and κ_i are the permittivity and conductivity of dispersed phase, ε_a and κ_a are the permittivity and conductivity of continuous phase. For such a system, Hanai's equation [53, 54] that was an extension of Wagner's equation [55] to high volume fractions along the Bruggman's effective medium approach was used:

$$\frac{\varepsilon^*-\varepsilon_i^*}{\varepsilon_a^*-\varepsilon_i^*}\left(\frac{\varepsilon_a^*}{\varepsilon^*}\right)^{1/3}=1-\phi \quad (3)$$

Using a systematic numerical method developed by Hanai for computing the phase parameters from the relaxation parameters ε_l, ε_h, κ_l, and κ_h in Table 1, the values of ε_i, κ_i, and ϕ are calculated and listed in Table 2. The permittivity of EG ε_a was considered to be a constant, 37.7, at the experimental temperature. The conductivity κ_a approximately changed from 0.55 to 0.78×10^{-4} S/cm, which was also listed in Table 2.

Figure 7 shows the dependence of the conductivity of constituent phases (dispersed phase (κ_i) and continuous phase (κ_a)) on the IL content. More interestingly, the size of "IL pool" linearly increase as the amount of IL increases [26], but it has no effect on κ_a because of the conductivity of ILs is too high in the system. In contrast, the conductivity of continuous phase κ_i slowly increased because the concentration of conductive ions ($[Bmim]^+$ and PF_6^-) increases with the increase in the IL content.

The diffusion of the interfacial ions arises from the well-known Maxwell–Wagner effect, and the relaxation time (τ_{MW}) can be estimated through the following equation [55]:

$$\tau_{MW}=\frac{2\varepsilon_i+\varepsilon_a+\phi(\varepsilon_i-\varepsilon_a)}{2\kappa_i+\kappa_a+\phi(\kappa_i-\kappa_a)}\varepsilon_0 \quad (4)$$

Figure 8 shows the dependence of the relaxation time of the calculated values τ_{MW} and experimental values τ (see Table 1) on the IL content. The calculated values τ_{MW} of different IL content were calculated to be in the range of 2.6–9.2 ns, which are in good agreement with the measured experimental values τ. This indicates that it is reasonable and credible to deal with the IL/EG subregion with the dielectric model of particle dispersion.

Table 2 Phase parameters of IL/EG microemulsions with different IL contents when the weight ratio of Triton X-100 was fixed at 62.5 %

Wt%(IL)	$\kappa_a(10^4\times$S/cm)	ε_i	κ_i ($10^4\times$S/cm)	ϕ	τ_{MW}/(ns)
2.5	0.55	7.74	1.32	0.53	9.18
5.0	0.58	7.88	1.56	0.57	7.58
7.5	0.63	7.98	2.24	0.58	5.34
10.0	0.66	8.09	2.66	0.61	4.41
12.5	0.70	8.19	3.31	0.63	3.49
15.0	0.74	8.29	3.73	0.66	3.04
17.5	0.78	8.37	4.23	0.68	2.63

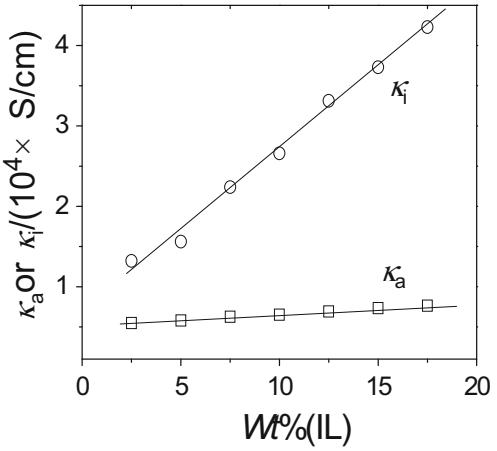

Fig. 7 Dependence of conductivity of constituent phases (dispersed phase (κ_i) and continuous phase (κ_a)) on the IL content when the weight ratio of Triton X-100 was fixed at 62.5 %

Structural transition of microemulsions

As the dielectric intensity $\Delta\varepsilon$ can provide some useful information on interfacial property of microemulsions in different phase regions, it is frequently used to obtain the microstructure of microemulsions [56]. Figure 5c shows the dependence of $\Delta\varepsilon$ on IL content, where three phase regions could be identified. When the IL content is below 18.6 %, more IL molecules entering into the micelle cores induce the increase of $\Delta\varepsilon$ with the increase of IL content. When the IL content is in the range from 18.6 to 30.0 %, $\Delta\varepsilon$ remains almost constant in B.C. subregion, probably because there is no obvious change of sum interface during the formation of channels in the region. When the IL content is exceeded 30 %, $\Delta\varepsilon$ begins

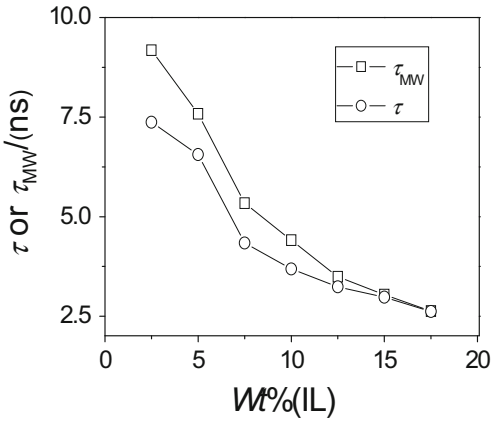

Fig. 8 Dependence of τ_{MW} and τ on the IL content when the weight ratio of Triton X-100 was fixed at 62.5 %

to fall with the increasing of IL content. This indicates that the decrease of phase interface of the EG droplets in EG/IL microemulsions. The dependence of $\Delta\varepsilon$ on IL content is in accordance with the result determined by the conductivity (Fig. 5a). From this point, the ILs-containing microemulsions were similar to the traditional aqueous microemulsions [52].

Conclusion

The dielectric behavior of EG/Triton X-100/[Bmim][PF_6] ternary nonaqueous system was investigated by DRS in a wide frequency range, and a remarkable relaxation caused by interface polarization was observed. By analyzing the dependence of dielectric intensity $\Delta\varepsilon$ and dc conductivity κ_1 on the IL content, the boundaries of EG/IL, B.C., and IL/EG subregions in single-phase region were accurately confirmed, which were well consistent with that characterized by other methods. These results inferred that IL content played a crucial role on the dynamics and phase behavior of nonaqueous microemulsions.

In the IL/EG micro-region, the internal properties of the constituent phase were calculated according to the Hanai equation, and some important structural information can be deduced from the phase parameters. In addition, the dielectric behavior has been interpreted in terms of interfacial polarization.

More importantly, this work shows the unique advantage and feasibility of detecting the microstructural characteristics of nonaqueous microemulsions system. In particular, the dynamic information and the structural properties obtained by DRS may provide some insights into the phase behavior of the microemulsions.

Acknowledgments Financial support of this work by the National Natural Scientific Foundation of China (No. 21173025, 21473012) and the Major Research Plan of NSFC (No. 21233003) are gratefully acknowledged.

References

1. Fanun M (2010) Microemulsions: Properties and applications, vol 144. CRC, New York, p 19
2. Martino A, Kaler EW (1990) Phase behavior and microstructure of nonaqueous microemulsions. J Phys Chem 94:1627
3. Martino A, Kaler E (1995) Phase behavior and microstructure of nonaqueous microemulsions. 2. Langmuir 11:779
4. Falcone RD, Correa NM, Biasutti MA, Silber JJ (2000) Properties of AOT aqueous and nonaqueous microemulsions sensed by optical molecular probes. Langmuir 16:3070
5. Durantini AM, Falcone RD, Silber JJ, Correa NM (2009) Effect of the constrained environment on the interactions between the surfactant and different polar solvents encapsulated within AOT reverse micelles. ChemPhysChem 10:2034
6. Durantini AM, Falcone RD, Silber JJ, Correa NM (2011) A new organized media: glycerol: N, N-dimethylformamide mixtures/AOT/n-heptane reversed micelles. The effect of confinement on preferential solvation. J Phys Chem B 115:5894
7. Lattes A, Rico I, De Savignac A, Samii A (1987) Formamide, a water substitute in micelles and microemulsions[xxx] structural analysis using a diels-alder reaction as a chemical probe. Tetrahedron 43:1725
8. Ray S, Moulik S (1994) Dynamics and thermodynamics of aerosol OT-aided nonaqueous microemulsions. Langmuir 10:2511
9. Attaphong C, Do L, Sabatini DA (2012) Vegetable oil-based microemulsions using carboxylate-based extended surfactants and their potential as an alternative renewable biofuel. Fuel 94:606
10. Gayet F, El Kalamouni C, Lavedan P, Marty JD, Brulet A, Lauth-de Viguerie N (2009) Ionic liquid/oil microemulsions as chemical nanoreactors. Langmuir 25:9741
11. Wasserscheid P (2006) Chemistry—Volatile times for ionic liquids. Nature 439:797
12. Rogers RD, Seddon KR (2003) Ionic liquids—Solvents of the future? Science 302:792
13. Eastoe J, Gold S, Rogers SE, Paul A, Welton T, Heenan RK, Grillo I (2005) Ionic liquid-in-oil microemulsions. J Am Chem Soc 127:7302
14. Greaves TL, Drummond CJ (2008) Ionic liquids as amphiphile self-assembly media. Chem Soc Rev 37:1709
15. Gao H, Li J, Han B, Chen W, Zhang J, Zhang R, Yan D (2004) Microemulsions with ionic liquid polar domains. Phys Chem Chem Phys 6:2914
16. Li N, Ya G, Zheng L, Zhang J, Yu L, Li X (2007) Studies on the micropolarities of bmimBF_4/TX-100/Toluene ionic liquid microemulsions and their behaviors characterized by UV-visible spectroscopy. Langmuir 23:1091
17. Gao Y, Wang S, Zheng L, Han S, Zhang X, Lu D, Yu L, Ji Y, Zhang G (2006) Microregion detection of ionic liquid microemulsions. J Colloid Interface Sci 301:612
18. Pramanik R, Sarkar S, Ghatak C, Rao VG, Sarkar N (2011) Ionic liquid containing microemulsions: Probe by conductance, dynamic light scattering, diffusion-ordered spectroscopy NMR measurements, and study of solvent relaxation dynamics. J Phys Chem B 115:2322
19. Li J, Zhang JL, Gao H, Han B, Gao L (2005) Nonaqueous microemulsion-containing ionic liquid bmim PF_6 as polar microenvironment. Colloid Polym Sci 283:1371
20. Rojas O, Tiersch B, Rabe C, Stehle R, Hoell A, Arlt B, Koetz J (2013) Nonaqueous microemulsions based on N, N′-alkylimidazolium alkylsulfate ionic liquids. Langmuir 29:6833
21. Harrar A, Zech O, Klaus A, Bauduin P, Kunz W (2011) Influence of surfactant amphiphilicity on the phase behavior of IL-based microemulsions. J Colloid Interface Sci 362:423
22. Fu C, Zhou H, Wu H, Chen J, Kuang Y (2008) Research on electrochemical properties of nonaqueous ionic liquid microemulsions. Colloid Polym Sci 286:1499
23. Li N, Zhang S, Zheng L, Gao Ya YL (2008) Second virial coefficient of bmimBF4/Triton X-100/ cyclohexane ionic liquid microemulsion as investigated by microcalorimetry. Langmuir 24:2973
24. Gao Y, Zhang J, Xu HY, Zhao XY, Zheng LQ, Li XW, Yu L (2006) Structural studies of 1-butyl-3-methylimidazolium tetrafluoroborate/TX-100/p-xylene ionic liquid microemulsions. ChemPhysChem 7:1554
25. Wei J, Su B, Liang R, Xing H, Bao Z, Yang Q, Yang Y, Ren Q (2012) Ionic liquid bmimCl/formamide mixture as the polar phase of nonaqueous microemulsions. Colloids Surf A 414:82
26. Cheng S, Fu X, Liu J, Zhang J, Zhang Z, Wei Y, Han B (2007) Study of ethylene glycol/TX-100/ionic liquid microemulsions. Colloids Surf A 302:211
27. Gao Y, Li N, Hilfert L, Zhang S, Zheng L, Yu L (2009) Temperature-induced microstructural changes in ionic liquid-based microemulsions. Langmuir 25:1360
28. Foster KR, Epstein BR, Jenin PC, Mackay RA (1982) Dielectric studies on nonionic microemulsions. J Colloid Interface Sci 88:233
29. Ponton A, Bose T, Delbos G (1991) Dielectric study of percolation in an oil—Continuous microemulsion. J Chem Phys 94:6879

30. Feldman Y, Kozlovich N, Alexandrov Y, Nigmatullin R, Ryabov Y (1996) Mechanism of the cooperative relaxation in microemulsions near the percolation threshold. Phys Rev E 54:5420
31. Tanaka R, Shiromizu T (2001) Stepwise process forming AOT W/O microemulsion investigated by dielectric measurements. Langmuir 17:7995
32. Bordi F, Cametti C (2001) Occurrence of an intermediate relaxation process in water-in-oil microemulsions below percolation: the electrical modulus formalism. J Colloid Interface Sci 237:224
33. Cametti C (2010) Dielectric spectra of ionic water-in-oil microemulsions below percolation: Frequency dependence behavior. Phys Rev E 81:031403
34. Middleton MA, Schechter RS, Johnston KP (1990) Dielectric properties of anionic and nonionic surfactant microemulsions. Langmuir 6:920
35. Feldman Y, Kozlovich N, Nir I, Garti N (1997) Dielectric spectroscopy of microemulsions. Colloids Surf A 128:47
36. Asami K (2005) Dielectric relaxation in a water–oil-Triton X-100 microemulsion near phase inversion. Langmuir 21:9032
37. Schrödle S, Buchner R, Kunz W (2005) Percolating microemulsions of nonionic surfactants probed by dielectric spectroscopy. ChemPhysChem 6:1051
38. He K, Zhao K, Chai J, Li G (2007) Dielectric analysis of the APG/*n*-butanol/cyclohexane/water nonionic microemulsions. J Colloid Interface Sci 313:630
39. Lian Y, Zhao K (2011) Study of micelles and microemulsions formed in a hydrophobic ionic liquid by a dielectric spectroscopy method. I. Interaction and percolation. Soft Matter 7:8828
40. Lian Y, Zhao K (2011) Dielectric analysis of micelles and microemulsions formed in a hydrophilic ionic liquid. I. Interaction and percolation. J Phys Chem B 115:11368
41. Peyrelasse J, Boned C, Saidi Z (1989) Percolation phenomenon in waterless microemulsions. Prog Colloid Polym Sci 79:263
42. Schwan HP (1960) Determination of biological impedances. In: Nastuk WL (ed) Physical techniques in biological research, vol 6. Academic, New York, p 323
43. Cole KS, Cole RH (1941) Dispersion and absorption in dielectrics I. Alternating current characteristics. J Chem Phys 9:341
44. Jiménez M, Arroyo F, van Turnhout J, Delgado A (2002) Analysis of the dielectric permittivity of suspensions by means of the logarithmic derivative of its real part. J Colloid Interface Sci 249:327
45. Clausse M, Peyrelasse J, Heil J, Boned C, Lagourette B (1981) Bicontinuous structure zones in microemulsions. Nature 293:636
46. Eicke HF, Borkovec M, Dasgupta B (1989) Conductivity of water-in-oil microemulsions: a quantitative charge fluctuation model. J Phys Chem 93:314
47. Maitra A, Mathew C, Varshney M (1990) Closed and open structure aggregates in microemulsions and mechanism of percolative conduction. J Phys Chem 94:5290
48. Hait S, Sanyal A, Moulik S (2002) Physicochemical studies on microemulsions. 8. The effects of aromatic methoxy hydrotropes on droplet clustering and understanding of the dynamics of conductance percolation in water/oil microemulsion systems. J Phys Chem B 106: 12642
49. Zhang X, Chen Y, Liu J, Zhao C, Zhang H (2012) Investigation on the structure of water/AOT/IPM/alcohols reverse micelles by conductivity, dynamic light scattering, and small angle X-ray scattering. J Phys Chem B 116:3723
50. Gao Y, Li N, Li X, Zhang S, Zheng L, Bai X, Yu L (2008) Microstructures of micellar aggregations formed within 1-butyl-3-methylimidazolium type ionic liquids. J Phys Chem B 113:123
51. Rao VG, Mandal S, Ghosh S, Banerjee C, Sarkar N (2012) Aggregation behavior of Triton X-100 with a mixture of two room-temperature ionic liquids: can we identify the mutual penetration of ionic liquids in ionic liquid containing micellar aggregates? J Phys Chem B 116:13868
52. Chen K, Zhao K (2014) Dielectric relaxation behavior of ternary systems of water/toluene/Triton X-100: the effects of water and oil contents on microemulsion structure. Colloid Polym Sci 292:557
53. Hanai T (1968) Electrical properties of emulsions. In: Sherman P (ed) Emulsion science. Academic, London, pp 354–477
54. Hanai T (1960) Theory of the dielectric dispersion due to the interfacial polarization and its application to emulsions. Colloid Polym Sci 171:23
55. Wagner K (1914) The after effect in dielectrics. Arch Electrotech 2: 378
56. Hanai T, Sekine K (1986) Theory of dielectric relaxations due to the interfacial polarization for two-component suspensions of spheres. Colloid Polym Sci 264:888